OpenNano 14 (2023) 100186

Contents lists available at ScienceDirect

OpenNano

journal homepage: www.elsevier.com/locate/onano

Enhanced skin delivery of vismodegib-loaded rigid liposomes combined with ethosomes

E.T. Aguayo Frías [a,b,1], D. Maza Vega [a,b,1], M.N. Calienni [a,b,c,d], C. Lillo [c,d,e], D.S. Vazquez [b,f], S.d.V. Alonso [a,b], J. Montanari [a,c,d,g,*]

[a] Laboratorio de Bio-Nanotecnología, Departamento de Ciencia y Tecnología, Universidad Nacional de Quilmes, Bernal, Buenos Aires 1876, Argentina
[b] Grupo de Biología Estructural y Biotecnología (GBEyB), IMBICE (CONICET CCT-La Plata), Buenos Aires 1906, Argentina
[c] Laboratorio de Nanosistemas de Aplicación Biotecnológica (LANSAB), Universidad Nacional de Hurlingham, Av. Vergara 2222 (B1688GEZ), Villa Tesei, Buenos Aires, Argentina
[d] Comisión de Investigaciones Científicas de la Provincia de Buenos Aires (CIC). Calles 60 y 118 (1900) La Plata, Buenos Aires, Argentina
[e] Instituto de Investigaciones Fisicoquímicas Teóricas y Aplicadas (INIFTA), Facultad de Ciencias Exactas, UNLP-CONICET, CC16 Suc 4 (1900), La Plata, Buenos Aires, Argentina
[f] Departamento de Ciencia y Tecnología, Universidad Nacional de Quilmes, Bernal, Buenos Aires 1876, Argentina
[g] Consejo Nacional de Investigaciones Científicas y Técnicas (CONICET), Ciudad Autónoma de Buenos Aires 1425, Argentina

ARTICLE INFO

Keywords:
Ethosomes
Liposomes
Drug delivery
Vismodegib

ABSTRACT

Vismodegib, first approved in 2012 for the treatment of basal cell carcinoma, is an inhibitor of the Hedgehog signaling pathway that becomes active in certain tumors. However, its secondary effects after oral administration and systemic distribution are severe. In this study, we loaded vismodegib into conventional liposomes, which are typically unable to penetrate the stratum corneum barrier effectively after topical application. We studied its skin penetration when co-administered with empty ethosomes, aimed at transiently disrupting the skin impermeability. The drug was successfully recovered from the deeper viable epidermal layers in an *in vitro* model. The preparation method for the liposomal formulation is reproducible and relatively straightforward to scale up. Furthermore, it involves the use of biocompatible lipids, thus avoiding the utilization of potentially risky compounds.

1. Introduction

Topical drug administration becomes particularly interesting when the therapeutic target is within the skin. Nanotechnology provides tools for designing site-specific delivery strategies that enable the use of minimal drug quantities, thereby maximizing therapeutic efficacy and diminishing systemic distribution to mitigate associated side effects [1]. Liposomes, which consist of phospholipid bilayers forming spherical structures, have been extensively studied as nanotechnological carriers for protecting and delivering active ingredients over the last few decades. They find application in a wide range of fields, including cosmetics, food, and pharmaceuticals. Notably, the first approved nanodrug, Ambisome [2], falls under the category of liposomal applications in the

* Corresponding author at: Laboratorio de Nanosistemas de Aplicación Biotecnológica (LANSAB), Universidad Nacional de Hurlingham, *Av.* Vergara 2222 (B1688GEZ), Villa Tesei, Buenos Aires, Argentina.
E-mail address: jorge.montanari@unahur.edu.ar (J. Montanari).
[1] These authors contributed equally to this work.

https://doi.org/10.1016/j.onano.2023.100186
Received 24 June 2023; Received in revised form 26 August 2023; Accepted 29 August 2023
Available online 30 August 2023

pharmaceutical sector. However, their effectiveness is limited for topical cutaneous application when dealing with the impermeable barrier of intact skin. This barrier function is attributed to the *stratum corneum* (SC), a layer composed of terminally differentiated cells called corneocytes. These cells lack nuclei, are rich in keratin, and possess very narrow intercellular spaces. They are surrounded by a lipid matrix that is abundant in ceramides and other lipids, creating an extremely hydrophobic environment [3].

In response to this challenge, various carrier systems have been developed, such as transfersomes [4], which involve the addition of an edge activator to the liposomal membrane. This unique feature significantly decreases the elastic modulus, allowing transfersomes to navigate through exceedingly narrow channels within the SC. This movement is propelled by dehydration pressure [5]. Another extensively investigated carrier is the ethosome [6], wherein a specific ratio of ethanol is incorporated into the lipid membrane [7]. Ethanol has the capability to induce temporary disruptions in the impermeability of the SC, thereby rendering the environment more fluid and generating larger spaces within corneocytes. These spaces are subsequently utilized by the ethosomes to penetrate the skin [8, 9]. Nonetheless, both nanocarriers have certain drawbacks: the primary edge activators used in transfersomes are expensive [7] and elicit concerns regarding their potential carcinogenic properties [10,11]. Similarly, the low yield and product losses encountered during the transition from organic to aqueous media compromise the economic viability of ethosome production, making it challenging to achieve economic feasibility [12].

On the other hand, vismodegib (Vis), a molecule with low water solubility and a molecular weight of 421.3, is a first-in-class inhibitor of the Hedgehog signaling pathway (Hh). It is indicated for the treatment of specific advanced stages of basal cell carcinoma [13]. Approved by the FDA in 2012, it subsequently received approval from diverse regulatory agencies in various regions. The recommended oral dosage is 150 mg daily, but its usage is associated with the emergence of several moderate to severe side effects, some of which have led to the discontinuation of treatment by certain patients [14]. In recent years, there has been a growing focus on its administration through the topical cutaneous route [15–20].

In this study, we propose the combination of ethosomes and conventional liposomes to obtain a unified formulation. Here, empty ethosomes serve as facilitators to aid the penetration of conventional liposomes into the deeper layers of the skin, precisely targeting the regions where molecules like Vis exert their therapeutic effects. Therefore, in this study, the improvement of the Vis delivery system, encapsulated within conventional liposomes, achieved by combining it with empty ethosomes. This approach mitigates the challenges previously described with similar systems.

2. Materials and methods

2.1. Materials

Soybean phosphatidylcholine (SPC) was bought from Avanti® Polar Lipids (Alabaster, AL, USA), as well as the 23-(dipyrrometheneboron difluoride)−24-norcholesterol (commercially TopFluor® cholesterol, abbreviation TFC). Vismodegib was provided as Erivedge® by a donation from Roche S.A.Q. e I. (Ricardo Rojas, Argentina), that also provided a Vismodegib standard (2-chloro-N-(4-chloro-3-(pyridin-2-yl)phenyl)−4-(methylsulfonyl)benzamide, MW=421.3 g/mol). Optimal cutting temperature compound (OCT), Tween 80, merocyanine 540 (MC540), and 1,2-Dipalmitoyl-sn-glycero-3-phosphoethanolamine labeled with lissamine rhodamine B-Sulfonyl (DPPE-Rh) were purchased from Sigma-Aldrich (Buenos Aires, Argentina). Chloroform, HPLC-grade trifluoroacetic acid, and acetonitrile were from J.T.Baker® (Buenos Aires, Argentina). All other reagents used were of analytical grade.

2.2. Vismodegib extraction from commercially formulated capsules

As previously described [21], Vis was extracted from commercial capsules and quantified. The procedure involved extracting the capsule content with methanol (1 mL of solvent to every 4 mg of Erivedge®) through 1-minute vortexing, followed by the precipitation of excipients through centrifugation. The subsequent experiments employed the resulting supernatant. This approach yielded a recovery rate of 78.8 ± 7.2%. RP-HPLC analysis was conducted at 225 nm using a gradient of mobile phases comprising acetonitrile and trifluoroacetic acid. The analysis was performed on a Waters Alliance 2690 liquid chromatography system equipped with a Waters Alliance 2487 UV-detector (Milford, MA, USA) and an Agilent ZORBAX Eclipse XDB-C18 column (150 × 3.0 mm, 3.5 m particle size) (Santa Clara, CA, USA). The Clarity 2.3 Software (DataApex, Prague, Czech Republic) facilitated the analysis. A calibration curve was generated in triplicate using the standard ($Y = 203.5^{*}\ X - 8.997$; $R^2 = 0.9995$), covering a range of 0.1 to 10 μg/mL [17,21].

2.3. Liposome preparation

Vis-loaded conventional liposomes (L-Vis) were prepared following the methodology previously described [17]. Briefly, L-Vis were obtained by re-dispersing lipid films composed of Soybean Phosphatidylcholine (SPC). Initially, 60 mg of SPC was weighed and then combined with a solution of Vis in a mass ratio of 40:1.4, respectively. Lipids were dissolved in chloroform through vortex shaking at medium speed for 30 s. The resulting solution was subjected to evaporation using a rotary evaporator set at 40 °C and 120 rpm, ensuring complete chloroform evaporation and lipid film formation. Subsequently, the film was re-suspended in Tris–HCl buffer with a pH of 7.4 through vortex shaking, and the resultant conventional liposomes underwent an automatic extrusion process aimed at reducing their size and lamellarity. A LipexTM 10 mL extruder (Transferra Nanosciences Inc., Burnaby, BC, Canada) connected to a nitrogen tank was employed for the extrusion process. The liposomes underwent nine extrusion cycles through two stacked membranes featuring pores with a size of 100 nm. This procedure was carried out under a pressure of 1.8 MPa. Moreover, for fluorescence testing purposes, empty liposomes were labeled and designated as L-F. To achieve this, DPPE-Rh was used as a liposomal membrane marker.

The lipids and DPPE-Rh were co-solubilized at a molar ratio of 1:1000 (fluorophore to SPC). The sample was shielded from light until measurements were conducted.

2.4. Ethosome preparation

Flexible ethosomes (Eth) were synthesized with slight modifications to established techniques [22,23]. SPC was briefly dissolved in a solution containing ethanol and Tween 80. Subsequently, Vismodegib (with a SPC:drug mass ratio of 40:1.4) was dissolved within the mixture, and distilled water was gradually added drop by drop while continuously vortexed until opalescence ocurred. After the addition of water, the concentrations of SPC, ethanol, and Tween 80 were 2, 45, and 0.4% w/v, respectively. Using a T-18 digital Ultraturrax® (IKA-Werke GmbH & Co. KG, Staufen, Germany), the suspension was agitated for one minute at 11,500 rpm. Following this, the excess ethanol was removed by swirling at 700 rpm for 30 min. The resulting suspension was then filtered first through a 0.45 μm-pore syringe filter and subsequently through a 0.2 μm-pore syringe filter. Additionally, tagged Eth (Eth-F) were produced utilizing TFC (at a 1:500 molar ratio of fluorophore to SPC) as an ethosomal membrane marker for fluorescence tests. These preparations were safeguarded from light, following established protocols.

2.5. Size and zeta potential

A Nanozetasizer (Malvern, Malvern, UK) was used to assess the mean particle sizes and PdI (Polydispersity Index) of both liposomes and ethosomes through dynamic light scattering (DLS). Using the same equipment, the Z-potential was calculated.

2.6. Vis-liposome membrane interaction

The interaction of Vis with the liposomal membrane was assessed through two complementary methods: differential scanning calorimetry (DSC) and utilizing the merocyanine 540 (MC540) probe. The phase transition temperature (Tm) from gel to liquid crystalline state, along with the corresponding change in enthalpy (ΔHcal), for L-Vis and empty L liposomes were determined in duplicate using a DSC Q200 instrument (TA Instruments, USA). A temperature ramp ranging from -50 to 30 °C was executed at a rate of 10 °C/min, following a 10-minute isothermal hold at -50 °C. Samples weighing 5.4 mg were placed in TZero hermetic pans and sealed securely with their respective lids. The TA Universal Analysis software was employed to calculate the thermodynamic parameters. On the other hand, MC540 was utilized to investigate alterations in phospholipid packing within liposomes upon the incorporation of Vis. This was accomplished by monitoring changes in the absorbance maxima of the monomer and dimer forms of MC540 as the molecule transitions from an aqueous solution to a hydrophobic environment [24]. To this end, liposomal suspensions were diluted 1:300 in Tris–HCl buffer at pH 7.4. Subsequently, the suspensions were incubated with a 0.768 μM solution of the MC540 probe at a 1:200 molar ratio of MC540 to lipids. The mixture was allowed to incubate at room temperature for 2 min before absorbance measurements were taken using a UV-1603 UV–VIS Spectrophotometer Shimadzu (Shimadzu, Japan). To mitigate liposome scattering, a baseline correction was applied to each measurement, involving triplicate assays using L or L-Vis, respectively, without MC540. A hydrophobicity factor (HF) was calculated as the ratio of absorbance at 570 nm to that at 500 nm.

2.7. Fluorescence emission

To assess the fluorescence of L-F and Eth-F, emission spectra were recorded for suspensions of different concentrations (1:100 and 1:1000 dilutions of each one). The excitation wavelengths used were in accordance with literature values: 570 nm for rhodamine and 495 nm for TFC. To carry out this analysis, a FluoroMate FS-2 spectrofluorometer (Scinco, Korea) was employed, utilizing a scan rate of 60 nm/min and a slit of 5 nm. Subsequently, the emission of each probe was examined in a 1:1 mixture of both suspensions. This was done to evaluate the signals independence from one another.

2.8. Skin penetration assays

2.8.1. Skin preparation and Saarbrücken penetration model use

To evaluate the skin penetration of the formulations, the Saarbrücken Penetration Model (SPM) [25] was employed. All skin-related protocols received approval from the Ethical Committee of the National University of Quilmes (project identification code:

Table 1
Tested formulations using the SPM.

Formulation	Volume (μl:μl)	Molar lipid ratio (mol:mol)
L-F (F1)	0:25 (Eth-F:L-F) [+25 μl of buffer]	0:1
Eth-F:L-F (F2)	25:25 (Eth-F:L-F)	1:2
Eth-F:L-F (F3)	10:40 (Eth-F:L-F)	1:10
Eth-F:L-F (F4)	40:10 (Eth-F:L-F)	2:1
Control skin (F5)	0:0 (Eth-F:L-F) [+50 μl of buffer]	–
Eth-F (F6)	25:0 (Eth-F:L-F) [+25 μl of buffer]	1:0

CE-UNQ N°1/2019, dated 04/29/2019), Argentina, and were carried out in adherence to the Code of Ethics of the World Medical Association. Skin samples came from healthy patients who had undergone esthetic surgery. These samples were then prepared for experimentation by eliminating the adipose hypodermal tissue, washing them with buffer pH 7.4, and subsequently freezing them at −20 °C while wrapped in aluminum foil into ziplock bags [26]. For the experimental setup, skin discs measuring 5 cm^2 were extracted from the specimens and placed within SPM teflon devices. These discs were oriented with the SC facing upwards and a filter paper was positioned at the bottom, saturated with Tris–HCl buffer to replicate the transdermal humidity gradient. The samples were incubated in a non-occlusive manner by applying 50 μl of suspension dropwise using a micropipette on the SC. Subsequently, they were placed in a 37 °C incubator for the designated time. Each formulation under each condition was tested in triplicate. An overview of the various formulations tested can be found in Table 1.

2.8.2. Skin distribution fluorescence assays

L-F and Eth-F aliquots were mixed in different proportions, as displayed in Table 1, reaching a final volume of 50 μl within plastic microtubes. In the case of control samples, buffer was added. Following the incubation period, specific samples underwent the tape stripping technique [27]. In this method, skin specimens were affixed to a polypropylene base using metal pins. The skin discs were cleansed with cotton to eliminate any residual formulations that had not penetrated. Subsequently, twenty pieces of adhesive tape were sequentially applied to the specimen with a weight of 2 kg for 10 s each. After removal, a layer of the SC was collected. The collected tapes were categorized into groups representing the shallow, middle, and deep SC (tapes 1–3, 4–10, and 11–20, respectively). The section of skin beneath the SC, corresponding to the viable epidermis and dermis (VED), was ground and collected in a fourth tube for each sample. Tapes and VED samples were subjected to extraction using a mixture of water and ethanol (1:1 v/v) with mechanical stirring in an orbital shaker at 37 °C for 1 h. Fluorescence intensity for both probes was measured based on the emission maxima following the earlier specified excitation conditions. For the best-performing formulation, additional samples were examined using fluorescence microscopy on a Cytation 5 (BioTek Instruments, USA). In this case, after incubation, the samples were embedded in OCT, frozen, and sliced into 15 μm-thick sections using a cryomicrotome (Leica CM 1850, Leica, Wetzlar, Germany) at -20 °C [21].

2.9. Vis penetration

Upon identifying the optimal combination of L and Eth formulations (1-hour incubation and a 1:2 molar lipid ratio), the selected mixture of L-Vis and Eth was applied to skin samples as previously described, followed by tape stripping. To extract Vis from both the tapes and VED samples, DMSO was employed. Subsequently, the concentration of Vis was determined through RP-HPLC utilizing a UV-detector at a wavelength of 225 nm. The conditions for this analysis were consistent with those detailed earlier [17]. Peak areas corresponding to the retention time of Vis were integrated, and Vis concentration was calculated using the previously described calibration curve.

2.10. Statistical analysis

The data were analyzed after confirming normal distribution through the Shapiro-Wilk test. Homoscedasticity was also verified using the F-test to compare variances. The Student's *t*-test was used for statistical analysis when only two groups were compared. One-way or Two-way ANOVA and Tukey's multiple comparisons tests were employed when comparing more than two sets of data. Only values with $p < 0.05$ were considered statistically significant. The analyzes were performed using GraphPad Prism 8.0.1 software (GraphPad Inc.).

3. Results and discussion

3.1. Size and zeta potential

The hydrodynamic size (Z-average), PdI and Z-potential values of the formulations were assessed using DLS. The data in Table 2 are shown as mean ± SD ($n = 3$). Notably, fluorescent vesicles exhibited no significant differences compared to their non-tagged counterparts (data not shown). The L-Vis formulation exhibited a larger size than the empty L. This could be attributed to the incorporation of Vis into the liposomal membrane. Nevertheless, the elevated PdI suggests that size reduction might be possible through additional extrusion cycles if deemed necessary, since it has been noted that approximately 20 extrusion cycles are sufficient for nearly any type of liposomal suspension to achieve a uniform size [28]. The zeta potential of L-Vis was also measured, yielding a value of −16.4 ± 1.91 mV. This indicates a negative surface charge on the liposomes, a feature attributed to the lipid composition of the liposomal membrane [24]. This surface charge enables the prediction of favorable stability for the formulation, guarding against rapid aggregation or

Table 2
DLS and Z-potential measurements of L, Eth, and L-Vis, displaying results from a $n = 3$ ± SD.

Formulation	Z-average	PdI	Z-pot (mV)
L	140.5 ± 4.0	0.084 ± 0.018	−16.2 ± 0.4
Eth	102.9 ± 2.2	0.122 ± 0.026	−18.0 ± 1.0
L-Vis	233.6 ± 7.1	0.271 ± 0.021	−17.6 ± 0.2

coalescence. The results obtained from DLS and Z-pot for the different nanosystems are consistent with the expected values according to the bibliography [19,22].

3.2. Vis-liposome membrane interaction

3.2.1. MC50 probe analysis

The MC540 probe is a useful tool for investigating the molecular arrangement of phospholipids within lipid membranes. This can be achieved by measuring the absorbance spectra within the visible range or assessing the fluorescence properties. The behavior of the probe as a monomer is manifested through its partition between polar and nonpolar environments, which in this context corresponds to the outer aqueous phase and the liposomal membrane, respectively [17,29]. The HF of MC540 is indicative of the extent to which hydrophobic sites are exposed and the organization of the liposomal surface. Incorporation of Vis led to a reduction in the HF of L from 2.055 ± 0.058 (empty L) to 1.654 ± 0.043 (L-Vis). This decrease in HF suggests that a greater number of MC540 monomers reside in the hydrophilic environment compared to the hydrophobic one. A comparison of these findings with the HF values reported by Calienni et al., 2019 for Vis-loaded transfersomes (T-Vis) [17], where the matrix also includes an edge activator, reveals an inversion of this relationship.

3.2.2. Differential scanning calorimetry (DSC)

The thermotropic profiles obtained from the DSC analysis of L and L-Vis (Fig. 1) showed two endothermic peaks, one close to 0 °C corresponding to the melting of the aqueous medium and another, below 0 °C. Notably, no significant disparity was observed in the phase transition temperature between L and L-Vis, with values of -21.90 and -21.93 °C, respectively. Likewise, the enthalpy also exhibited negligible variation (Table 3).

The DSC outcomes detailed by Calienni et al., 2019 [17] for T-Vis compared to empty transfersomes (T) demonstrated a similarity in transition temperature, aligning with the observations derived from the DSC analysis of L-Vis versus L. In that study, a noticeable alteration was detected in terms of enthalpy. However, it is worth noting that this change in enthalpy was not evident when comparing L with L-Vis in the current study. The difference between L-Vis and T-Vis is the presence of the edge activator within the membrane. Therefore, it appears that the inclusion of Vis in L does not bring about any noticeable modification in the thermotropic behavior of the liposomal membrane. One possible explanation for this observation could be that, even though previous research suggests that Vis is indeed incorporated into the membrane, at the concentration employed, this interaction might not yield substantial consequences as revealed by DSC analysis. In fact, the modification of parameters in this type of liposome analysis has been shown to be concentration-dependent [30]. However, changes in the enthalpy studied by DSC did emerge when the bilayers incorporated an additional agent, as in the case of T which present the edge activator sodium cholate [17]. Nevertheless, in the aforementioned case, stability and structure, as assessed by several methods, remained unaltered. In the context of the current study, the appearance of the formulations throughout the experiments (derived from the same batches) and the prediction of their Z-potential values both provide indications that the formulations are likely to exhibit stability.

3.3. Fluorescence and skin penetration

3.3.1. Fluorescence emission

Fluorescence spectra of the labeled formulations were obtained (Fig. 2). In the left panel, at the emission wavelength corresponding to the maximum intensity for a 1:100 dilution of Eth-F, the emitted fluorescence was notably greater compared to that generated by a sample of the same formulation with a lower concentration. Additionally, the emitted fluorescence from the 1:100 Eth-F dilution exceeded that of the probe originating from the F1 formulation (labeled with a distinct fluorophore). Similarly, in the right panel, the fluorescence intensity at the peak maximum for F1 was significantly higher compared to the intensity for the corresponding lower

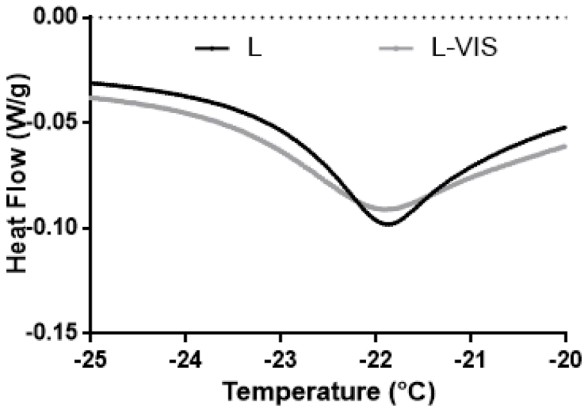

Fig. 1. Differential scanning calorimetry of empty and vismodegib-loaded liposomes.

Table 3
Thermodynamic parameters of the phase transition of L and L-Vis followed by DSC.

Sample	T_m (°C)[a]	ΔH_{cal} ($\frac{J}{g}$)[b]
L	−21.90	8.862
L-Vis	--21.93	8.574

[a] Temperature corresponding to the minimum of the calorimetric peak.
[b] Calorimetric enthalpy calculated as the area under the curve.

concentration. Furthermore, the fluorescence intensity of F1 at that specific wavelength exceeded that of Eth-F. This allowed for concurrent utilization of both probes, with the understanding that the emission would be specific to each probe. Moreover, the fluorescence emission was contingent on concentration, facilitating the distinction between a substantial presence of each probe and its mere detection threshold.

3.3.2. Skin penetration of fluorescent formulations

Fig. 3 illustrates the signal of labeled liposomes F1 recovered from various skin layers following a 1-hour incubation. Notably, in the VED region, the targeted zone of this system, the F1 signal displayed no significant deviation from the 0:0 formulation. This suggests that the observed signal can be attributed to skin autofluorescence. However, F2 and F4 exhibited considerable distinctions when compared to F1 and F5 controls. These formulations, combining co-incubated liposomes with ethosomes, led to an increased presence of the fluorescent marker within the VED region. In Fig. 4, where the fluorescence of the ethosome marker (Eth-F) was evaluated in the same samples, similar performance trends were evident across the formulations.

In Fig. 5, the cumulative fluorescence is depicted as the sum of signal intensities from each tape group of the SC in addition to the corresponding VED region. This assay was made for two different incubation durations: 40 min and 1 hour. The tested formulation was F2, which demonstrated the most promising outcomes from prior incubations. The penetration profile of F2 exhibited a notable increase when skin explants were incubated for 1 hour, suggesting that prolonged incubation times result in enhanced penetration. This phenomenon has been observed in previous studies for different formulations [17]. Given these findings, an incubation duration of 1 hour was chosen for the L-Vis studies. This decision is supported by the understanding that increased formulation penetration implies heightened drug bioavailability within the skin region housing its intended targets.

F2 was also chosen for examination using fluorescence microscopy. Fig. 6 presents the topical penetration of both nanosystems when the skin explants are subjected to incubation with the formulation. The obtained results illustrate that the delivery vehicles effectively traverse the SC, reaching both the VED. This observation aligns with the earlier findings highlighted in the fluorescence measurements after tape stripping (Fig. 3). All the skin penetration results presented here are particularly interesting since it is well-known that conventional liposomes like these, due to their rigidity, tend to fail in traversing the stratum corneum, leading to accumulation on the skin surface [31].

3.3.3. Vis recovery from skin

After the quantification of Vis collected from each tape group and the VED, the results were categorized into two distinct data groups. One set of data encompassed the penetration within the SC, which involved the summation of Vis retrieved from the 20 adhesive tapes. The second set of data pertained to the VED region.

As depicted in the upper panel of Fig. 7, the L-Vis formulation without the presence of Eth exhibited an inability to traverse the SC, leading to its retention within this layer. Consequently, the quantification of Vis content present in the adhesive tapes yielded values ranging from 20 to 28 μg, which constitutes nearly 80% of the initially administered Vis within the L. The ineffectiveness of conventional liposomes as a topical delivery vehicle is further highlighted by the absence of Vis within the VED region. Therefore, the release of Vis would be constrained solely to the SC, failing to reach the *stratum basale* where its intended therapeutic target is located.

Upon comparing these findings with those of the Eth + L-Vis formulation, the graph illustrates the presence of Vis in the adhesive

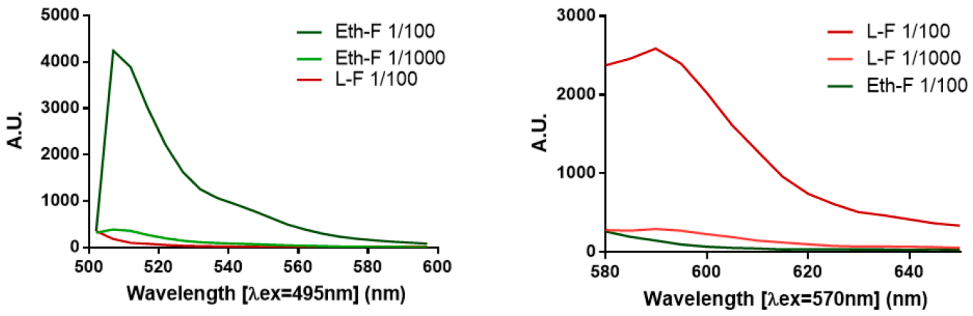

Fig. 2. Emission spectra of both probes in the nanosystems, (a) λ_{exc} = 495 nm (TFC) and (b) λ_{exc} = 570 nm (DPPE-Rho).

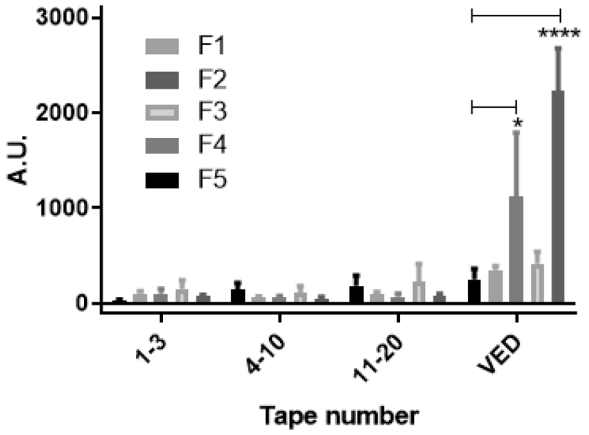

Fig. 3. Penetration profiles of L (mean ± SEM, $n = 3$) after excitation at 570 nm. Two-way ANOVA with Tukey's multiple comparisons test (* = $p < 0.05$; **** = $p < 0.0001$) was used to assess significance.

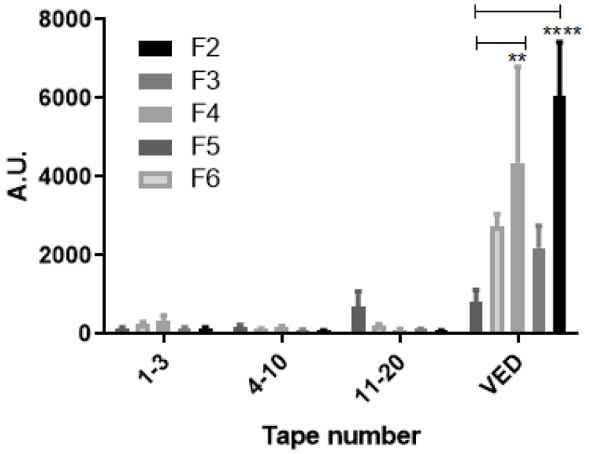

Fig. 4. Penetration profiles of Eth (mean ± SEM, $n = 3$) after excitation at 495 nm. Two-way ANOVA with Tukey's multiple comparisons test (** = $p < 0.01$; **** = $p < 0.0001$) was used to assess significance.

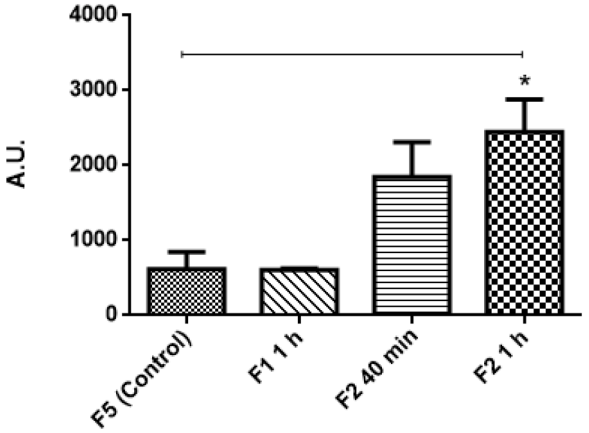

Fig. 5. Cumulative fluorescence assessed under varying incubation times. Significance analysis was conducted using One-way ANOVA with Tukey's multiple comparisons test (* = $p < 0.05$).

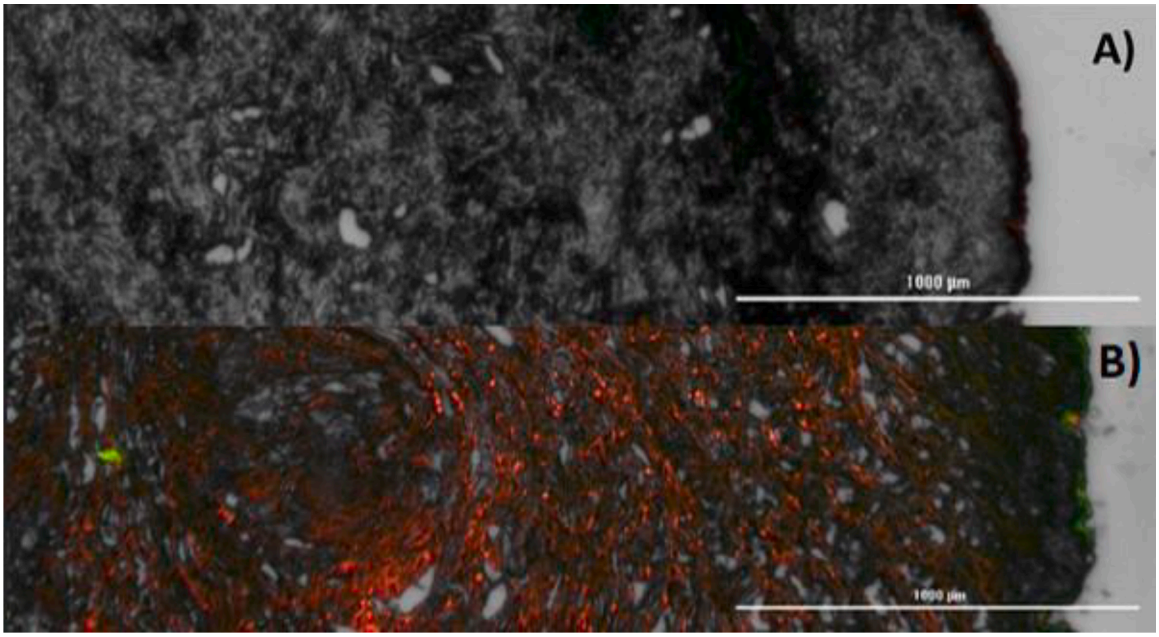

Fig. 6. Fluorescence images of transversal sections of skin. (A) Control without formulations. (B) Sample incubated with formulation F2 (label from liposome is shown in red, while label from ethosomes is indicated in green).

tapes attributed to the SC, albeit to a lesser degree compared to the L-Vis formulation devoid of Eth. On the right side of the figure, using the same scale, the quantified Vis content in the VED region, where its therapeutic target resides, is depicted. To enhance clarity regarding the differences in Vis concentration within the VED for each formulation, the same data are presented separately on a larger scale in the lower panel of Fig. 7. Notably, when Vis is administered using the Eth + L-Vis formulation, significant differences in Vis content within the VED region are evident in comparison to the scenario where Vis is administered without the co-administration of Eth (L-Vis). In the latter case, the presence of Vis in the VED is undetectable. This observation aligns with the findings from the fluorescence experiments and is consistent with the previously cited literature [31].

In both figures, the assessment of free Vis within the skin was integrated as a control, following a penetration test using the same protocol previously conducted by the research group [17]. Free Vis had been applied to the skin via a DMSO solution. To facilitate result comparison, a correction factor was introduced in relation to the total Vis mass applied. The average determined Vis value (2.561 µg) surpassed that of the free Vis formulation (0.545 µg) by a factor of 4.7, with this discrepancy being statistically significant. Consequently, the topical penetration model utilizing L as a Vis carrier and Eth as permeation enhancer exhibits an enhanced Vis administration performance when contrasted with the topical administration of free Vis. Until now, the only reported instance of Vis entering the skin through a liposomal system had been achieved with transfersomes [17], which had yielded similar differences compared to the penetration of the free drug. These results are promising, as models utilizing skin explants for *in vitro/ ex vivo* assays have demonstrated a strong correlation with *in vivo* penetration, making them reliable predictors [32].

4. Conclusions

The utilization of empty ethosomes as penetration enhancers for topically applied rigid conventional liposomes loaded with vismodegib and other compounds is a significant advancement. This collaborative effect, achieved by integrating distinct entities within a single formulation, holds intrinsic interest. In the case of vismodegib, this approach offers a potential alternative for delivering the drug to the deep epidermal layers through the use of harmless, biocompatible compounds and easily scalable carriers. However, it is crucial to further assess the specific impact of this system on enhancing vismodegib delivery and its subsequent therapeutic effectiveness through *in vivo* models. The prospect of employing ethosomes as permeation enhancers that actively facilitate the entry of other rigid nanostructures is a promising avenue for exploration. This approach may prove especially beneficial for the skin-friendly delivery of various rigid nanomedicines and nanoparticulate agents, and it may help to avoid crucial limitations of transfersomes as their lack of stability and scalability [33], and it also offers the potential to avoid the use of certain edge activators which are currently under investigation for their potential carcinogenicity [34]. Future research should delve into the potential applications and advantages of this approach in diverse contexts.

CRediT authorship contribution statement

E.T. Aguayo Frías: Investigation, Validation, Formal analysis, Data curation, Writing – original draft, Visualization. **D. Maza**

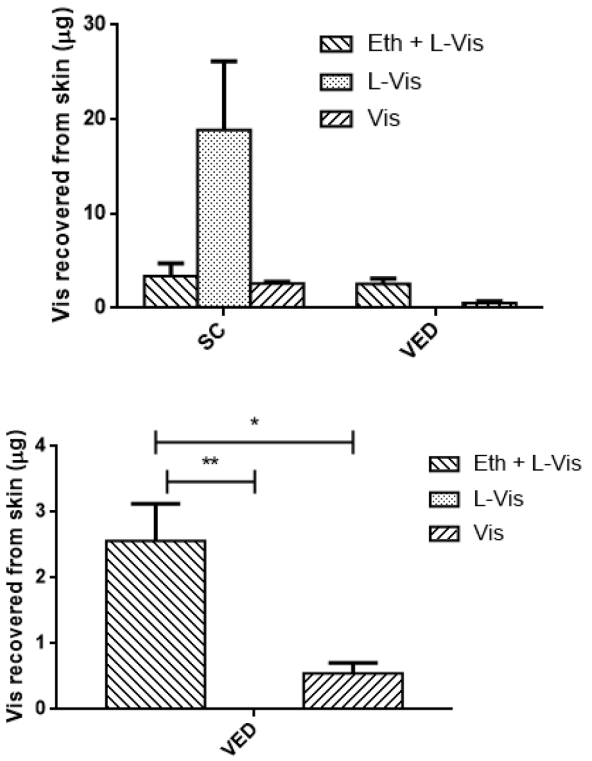

Fig. 7. The recovery of Vis from the skin through tape stripping after a 1 h incubation using formulations containing Eth co-loaded with L-Vis, L-Vis, and free Vis. The incubation was carried out at 36 °C on the SPM. The mass of Vis retrieved from both the stratum corneum (SC) and the viable epidermis + dermis (VED) is presented as mean ± SD ($n = 4$). Significance analysis was conducted using One-way ANOVA with Tukey's multiple comparisons test (* = $p < 0.05$; ** = $p < 0.01$).

Vega: Investigation, Validation, Formal analysis, Data curation, Writing – original draft, Visualization. **M.N. Calienni:** Conceptualization, Validation, Resources, Data curation, Writing – original draft, Writing – review & editing, Visualization, Supervision, Funding acquisition. **C. Lillo:** Investigation, Data curation. **D.S. Vazquez:** Investigation. **S.d.V. Alonso:** Validation, Resources, Funding acquisition. **J. Montanari:** Conceptualization, Methodology, Validation, Formal analysis, Resources, Data curation, Writing – original draft, Writing – review & editing, Visualization, Supervision, Project administration, Funding acquisition.

Declaration of Competing Interest

The authors declare that they have no known competing financial interests or personal relationships that could have appeared to influence the work reported in this paper.

References

[1] D.M. Rata, A.N. Cadinoiu, L.I. Atanase, M. Popa, C.T. Mihai, C. Solcan, G. Vochita, Topical formulations containing aptamer-functionalized nanocapsules loaded with 5-fluorouracil-an innovative concept for the skin cancer therapy, Mater. Sci. Eng. C 119 (2021), 111591.
[2] J.P. Adler-Moore, R.T. Proffitt, Development, characterization, efficacy and mode of action of AmBisome, a unilamellar liposomal formulation of amphotericin B, J. Liposome Res. 3 (3) (1993) 429–450.
[3] J.M. Abdo, N.A. Sopko, S.M. Milner, The applied anatomy of human skin: a model for regeneration, Wound Med. 28 (2020), 100179.
[4] A. Kumar, Transferosome: a recent approach for transdermal drug delivery, J. Drug Deliv. Ther. 8 (5–s) (2018) 100–104.
[5] G. Cevc, G. Blume, Lipid vesicles penetrate into intact skin owing to the transdermal osmotic gradients and hydration force, Biochim. Biophys. Acta Biomemb. 1104 (1) (1992) 226–232.
[6] E. Touitou, N. Dayan, L. Bergelson, B. Godin, M. Eliaz, Ethosomes—novel vesicular carriers for enhanced delivery: characterization and skin penetration properties, J. Control. Release 65 (3) (2000) 403–418.
[7] D.K. Mishra, N. Balekar, V. Dhote, P.K. Mishra, Ethosomes: a novel carrier for dermal or transdermal drug delivery. Carrier-Mediated Dermal Delivery, Jenny Stanford Publishing, 2017, pp. 357–383.
[8] P. Verma, K. Pathak, Therapeutic and cosmeceutical potential of ethosomes: an overview, J. Adv. Pharm. Technol. Res. 1 (3) (2010) 274.
[9] D. Maza Vega, M.C. Izquierdo, P. Bucci, J. Montanari, Delivery en piel humana de sondas fluorescentes como análogos de fármacos lipofílicos e hidrofílicos nanoformulados en etosomas. XXVII Jornadas de Jovens pesquisadores: A Ciência e a Tecnologia na Produção de Inovação e Transformação Social, Universidade Federal de São Carlos, São Paulo, Brasil, 2019.
[10] Y.B. Gándola, C. Fontana, M.A. Bojorge, T.T. Luschnat, M.A. Moretton, D.A. Chiapetta, L. González, Concentration-dependent effects of sodium cholate and deoxycholate bile salts on breast cancer cells proliferation and survival, Mol. Biol. Rep. 47 (2020) 3521–3539.
[11] C. Bernstein, H. Holubec, A.K. Bhattacharyya, H. Nguyen, C.M. Payne, B. Zaitlin, H. Bernstein, Carcinogenicity of deoxycholate, a secondary bile acid, Arch. Toxicol. 85 (2011) 863–871.

[12] K.P. Jadhav, A. Kundan, K. Kapadnis, D. Shinkar, V. Pathan, A. Jadhav, Ethosomes as novel drug delivery system: a review, Int. J. Pharm. Sci. Rev. Res 62 (1) (2020) 173–182.
[13] A. Dlugosz, S. Agrawal, P. Kirkpatrick, Vismodegib pipeline pioneers, Nat. Rev. Drug Discov. 11 (2012) 437.
[14] A. Sekulic, M.R. Migden, A.E. Oro, L. Dirix, K.D. Lewis, J.D. Hainsworth, A. Hauschild, Efficacy and safety of vismodegib in advanced basal-cell carcinoma, N. Engl. J. Med. 366 (23) (2012) 2171–2179.
[15] C.M. Olsen, J.F. Thompson, N. Pandeya, D.C. Whiteman, Evaluation of sex-specific incidence of melanoma, JAMA Dermatol. 156 (5) (2020) 553–560.
[16] H.X. Nguyen, A.K. Banga, Enhanced skin delivery of vismodegib by microneedle treatment, Drug Deliv. Transl. Res. 5 (2015) 407–423.
[17] M.N. Calienni, C. Febres-Molina, R.E. Llovera, C. Zevallos-Delgado, M.E. Tuttolomondo, D. Paolino, J. Montanari, Nanoformulation for potential topical delivery of Vismodegib in skin cancer treatment, Int. J. Pharm. 565 (2019) 108–122.
[18] S.G. Kandekar, M. Singhal, K.B. Sonaje, Y.N. Kalia, Polymeric micelle nanocarriers for targeted epidermal delivery of the hedgehog pathway inhibitor vismodegib: formulation development and cutaneous biodistribution in human skin, Expert Opin. Drug Deliv. 16 (6) (2019) 667–674.
[19] M.N. Calienni, D. Maza Vega, C.F. Temprana, M.C. Izquierdo, D.E. Ybarra, E. Bernabeu, J Montanari, The topical nanodelivery of vismodegib enhances its skin penetration and performance *in vitro* while reducing its toxicity *in vivo*, Pharmaceutics 13 (2) (2021) 186.
[20] O.M. Sayed, F.I. Abo El-Ela, R.M. Kharshoum, H.F. Salem, Treatment of basal cell carcinoma via binary ethosomes of vismodegib: *in vitro* and *in vivo* studies, AAPS PharmSciTech 21 (2020) 1–11.
[21] D.E. Ybarra, M.N. Calienni, L.F.B. Ramirez, E.T.A. Frias, C. Lillo, S. del Valle Alonso, F.C. Alvira, Vismodegib in PAMAM-dendrimers for potential theragnosis in skin cancer, OpenNano 7 (2022), 100053.
[22] M. Rady, I. Gomaa, N. Afifi, M Abdel-Kader, Dermal delivery of Fe-chlorophyllin via ultradeformable nanovesicles for photodynamic therapy in melanoma animal model, Int. J. Pharm. 548 (1) (2018) 480–490.
[23] D. Paolino, G. Lucania, D. Mardente, F. Alhaique, M. Fresta, Ethosomes for skin delivery of ammonium glycyrrhizinate: *in vitro* percutaneous permeation through human skin and *in vivo* anti-inflammatory activity on human volunteers, J. Control. Release 106 (1–2) (2005) 99–110.
[24] M.N. Calienni, C.F. Temprana, M.J. Prieto, D. Paolino, M. Fresta, A.B. Tekinay, J. Montanari, Nano-formulation for topical treatment of precancerous lesions: skin penetration, *in vitro*, and *in vivo* toxicological evaluation, Drug Deliv. Transl. Res. 8 (2018) 496–514.
[25] U. Schaefer, H. Loth, An *ex-vivo* model for the study of drug penetration into human skin, Pharm. Res. 13 (366) (1996) b24.
[26] J. Montanari, C. Maidana, M.I. Esteva, C. Salomon, M.J. Morilla, E.L. Romero, Sunlight triggered photodynamic ultradeformable liposomes against Leishmania braziliensis are also leishmanicidal in the dark, J. Control. Release 147 (3) (2010) 368–376.
[27] M.C. Izquierdo, C.R. Lillo, P. Bucci, G.E. Gomez, L. Martínez, S.D.V. Alonso, J. Montanari, Comparative skin penetration profiles of formulations including ultradeformable liposomes as potential nanocosmeceutical carriers, J. Cosmet. Dermatol. 19 (11) (2020) 3127–3137.
[28] J.J. Carreras, W.E. Tapia-Ramirez, A. Sala, A. Guillot, T. Garrigues, A. Melero, Ultraflexible lipid vesicles allow topical absorption of cyclosporin A, Drug Deliv. Transl. Res. 10 (2020) 486–497.
[29] M. Marsanasco, S. Alonso, Stability of bioactive compounds in liposomes after pasteurisation and storage of functional chocolate milk, Int. J. Food Sci. Technol. (57) (2022) 361–369.
[30] M. Romero-Arrieta, E. Uria-Canseco, S. Perez-Casas, Simultaneous encapsulation of hydrophilic and lipophilic molecules in liposomes of DSPC, Thermochim. Acta (687) (2020), 178462.
[31] E.B. Souto, A.S. Macedo, J. Dias-Ferreira, A. Cano, A. Zielińska, C.M. Matos, Elastic and ultradeformable liposomes for transdermal delivery of active pharmaceutical ingredients (APIs), Int. J. Mol. Sci. 22 (2021) 9743.
[32] A. Salimi, H. Ghobadian, B.S. Makhmalzadeh, Dermal pharmacokinetics of rivastigmine-loaded liposomes: an *ex vivo–in vivo* correlation study, J. Liposome Res. 31 (3) (2021) 246–254.
[33] A. Guillot, M. Martínez-Navarrete, T. Garrigues, A. Melero, Skin drug delivery using lipid vesicles: a starting guideline for their development, J. Control. Release (325) (2023) 624–654.
[34] Y.B. Gándola, C. Fontana, M.A. Bojorge, T. Luschnat, M. Moretton, D. Chiapetta, S. Verstraeten, L. Gonzalez, Concentration-dependent effects of sodium cholate and deoxycholate bile salts on breast cancer cells proliferation and survival, Mol. Biol. Rep. 47 (2020) 3521–3539.